MECSOL 2019 - Proceedings of the 7th International Symposium on Solid Mechanics,
V. Tita, A. Ferreira, M.L. Ribeiro, A. Vieira and A.T. Beck (Editors), ABCM, Sao Carlos, SP, Brazil, April 15th to 17th, 2019

Multiaxial fatigue of steels with small defects

Pedro Vinícius Sousa Machado, Edgard Soares Pinto Neto, Marcos Venicius Soares Pereira, José Alexander Araújo

Department of Mechanical Engineering, Faculty of Technology, University of Brasília, Brasília, DF 70910-900, Brazil

Abstract: The goal of this research is to investigate the detrimental effect of artificial small holes on the fatigue strength of steel under multiaxial loading conditions. Such holes are said to simulate the presence of non-metallic inclusions, which are chemical compounds that appear during the manufacturing processes due to several reasons such as contamination and are known to be detrimental to the fatigue strength, as they behave as stress concentration elements. Therefore, to consider this effect in a multiaxial problem a correction to the Modified Wöhler Curve Model (MWCM) is going to be proposed. The correction is based on the parameter "square root of area" investigated by Murakami (1994), and to assess it, experimental multiaxial fatigue data available in the literature were considered. The results show good agreement between the proposed model and the experiments of multiaxial fatigue of steels containing small artificial holes simulating nonmetallic inclusions.

Keywords: nonmetallic inclusions, defective materials, multiaxial fatigue, small defects

INTRODUCTION

The $\sqrt{area}$ parameter and the fatigue strength of naturally defective steels

The detrimental effect of nonmetallic inclusions on the fatigue strength of steels has been well documented (Schönbauer and Yanase, 2016, Yamashita et al, 2018) and has recently been a subject of debate as the possible cause of failures in crankshafts of thermoelectric powerplants in Brazil. These nonmetallic inclusions are known to behave as small cracks in the sense that they considerably increase the stress gradient field in its vicinities. In Figure 1 a picture of a nonmetallic inclusion found in AISI 4140 steel.

Figure 1 - Picture of a nonmetallic inclusion in an AISI 4140 steel sample (Source: Author)

However, it can be impractical to calculate their stress concentration factor as their shape and geometry vary consistently. For this reason, Murakami (2002a) proposed the existence of nominal fatigue limit (σ_w with $R = -1$), for these materials, Eq. (1), which could be estimated from the material hardness and the square root of the area of the defect projected in the direction of maximum normal stress, $\sqrt{area}$. An analogous formulation also was proposed to predict the nominal torsional fatigue limit (τ_w with $R = -1$) of steels (Murakami, 2002b), Eq. (2):

$$\sigma_w = \frac{1.43(Hv + 120)}{\left(\sqrt{area}_{max}\right)^{\frac{1}{6}}} \tag{1}$$

$$\tau_w = \frac{0.93(Hv + 120)}{F\left(\frac{b}{a}\right)\left(\sqrt{area}_{max}\right)^{\frac{1}{6}}} \tag{2}$$

where

$$F\left(\frac{b}{a}\right) = 0.0957 + 2.11\left(\frac{b}{a}\right) - 2.26\left(\frac{b}{a}\right)^2 + 1.09\left(\frac{b}{a}\right)^3 - 0.196\left(\frac{b}{a}\right)^4. \tag{3}$$

the coefficient F being a shape factor, function of the inclusion's aspect ratio b/a, where a is half of its width and b is its depth. To measure $\sqrt{area}$ of an inclusion, first, one needs to cut a sample of steel in the direction normal to the maximum principal stress, polish and mirror finish it and then use a microscope to its measuring area. The $\sqrt{area}_{max}$ parameter, given in μm, is the maximum statistically predicted inclusion's $\sqrt{area}$ in the tested sample. It can be estimated by considering the statistics of extremes method (Murakami and Endo, 1993). However, this statistical method will not be necessary, as the data presently analyzed is from specimens that contained artificial holes, hence with known $\sqrt{area}_{max}$ on its surfaces.

The errors of fatigue limits provided by Eqs. (1) and (2) are reported to be generally lower than 10% for specimens containing nonmetallic inclusions or artificial, as long as $\sqrt{area}_{max} \leq 1000\ \mu m$ and the material hardness be between 70 and $720\ Hv$ (Murakami and Endo, 1994).

Despite its strength, these models become problematic once multiaxial cyclic loading is considered, especially if they are non-proportional, as the direction of the principal stresses' components may vary constantly. In these cases, the $\sqrt{area}$ becomes hard to define, as there is no fixed position for the plane perpendicular to the maximum principal stress component. There have been some attempts to solve this issue.

Nadot and Billaudeau (2006) have proposed a multiaxial fatigue model for materials containing small defects that had good results. They considered the stress distribution around an artificially introduced defect (drilled holes) and concluded that the gradient of hydrostatic part of the stress tensor of the stress around a defect controls the fatigue limit under multiaxial loading. Their model introduced the gradient of the hydrostatic stress in Crossland's criterion. However, this model relies on advanced finite element analysis technics to determine the stress field around each type of defect, because the material around many defect types experiences plastic deformation. Moreover, the model might not be completely adequate, because only one loading cycle was considered in the simulation to determine the stress field around a defect, despite the possibility of occurring plastic deformation during the entire fatigue life.

Also, Endo and Ishimoto (2006) estimated that fatigue failure under multiaxial loading would occur, if a linear combination of the principal stresses of the combined varying axial and torsional stresses ($\sigma_1 + \kappa\sigma_2$) reached the value of σ_w (Equation 1). However, the model they proposed does not consider an important factor of a fatigue problem: the amplitude of the loading. For this reason, it has inconsistencies, such as predicting failure by fatigue when very little or no cyclic loading is present.

METHODOLOGY

The Modified Wöhler Curve Model (MWCM)

A possible solution for the presented problem is to use the Modified Wöhler Curve Model (MWCM), which is a multiaxial fatigue model based on the critical plane approach (Susmel and Lazzarin, 2002). To select the critical plane, first one needs to calculate the shear stress loading history in each material plane. These planes are characterized by their normal unitary vector $\boldsymbol{n}$ (see Fig. 1). A material plane is any plane that passes through the material point that is being analyzed. The vector $\boldsymbol{n}$ can be defined by its spherical coordinates ϕ and θ. According to Cauchy's theorem, the stress vector $\boldsymbol{t}(t)$ results from applying $\boldsymbol{n}$ to the stress tensor $\boldsymbol{T}(t)$, that varies with time in a loading cycle. The stress vector $\boldsymbol{t}(t)$ has two components: the shear stress vector $\boldsymbol{\tau}(t)$ (parallel to the material plane) and the normal stress vector $\boldsymbol{\sigma}(t)$ (normal to the material plane) see Fig. 2. In the following set of equations, the described procedure is written in a mathematical form:

$$\boldsymbol{t}(t) = \boldsymbol{T}(t)\boldsymbol{n} \tag{4}$$

$$\boldsymbol{\sigma}(t) = \big((\boldsymbol{T}(t)\boldsymbol{n}).\boldsymbol{n}\big)\boldsymbol{n} \tag{5}$$

$$\boldsymbol{\tau}(t) = \boldsymbol{t}(t) - \boldsymbol{\sigma}(t) \tag{6}$$

The MWCM (Susmel and Lazzarin, 2002) considers that fatigue crack initiation damage depends on a combination of the maximum shear stress amplitude (τ_a) in a material plane and the maximum normal stress ($\sigma_{n,max}$) to this critical plane (defined by $\boldsymbol{n}(\phi_c, \theta_c)$):

$$\lambda \geq \tau_a(\theta_c, \phi_c) + \kappa \frac{\sigma_{n,max}}{\tau_a}(\theta_c, \phi_c) \tag{7}$$

where κ and λ are material constants that can be obtained from the fatigue limits under fully reversed push-pull (or rotating bending) (f_{-1}) and torsion (t_{-1}) tests. Failure will occur should this inequation does hold. The values κ and λ are:

$$\lambda = t_{-1} \qquad k = \frac{2t_{-1} - f_{-1}}{2} \tag{8}$$

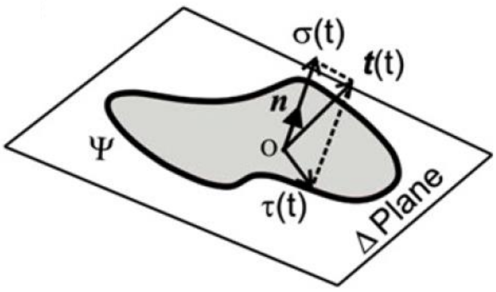

Figure 2 - Material plane Δ passing through a point of a specimen under multiaxial loading: its normal, $\boldsymbol{\sigma}(\boldsymbol{t})$, and shear, $\boldsymbol{\tau}(\boldsymbol{t})$, components of the loading history (Araújo et al., 2010)

The τ_a parameter is defined as the maximum shear stress amplitude, and the material plane where it occurs is the so called the critical plane. This parameter may be calculated in several ways, such as the classic Minimum Circumscribed Circle (MCC) (Bernasconi, 2001). However, the present work will compute it by the Maximum Rectangular Hull (MRH) algorithm (Araújo et al, 2011), which besides being very simple to implement, can take into account the effect of the non-proportional stress histories. In this method, the maximum shear stress amplitude is defined as half of the diagonal of the maximum rectangular hull that envelops the entire history of the shear stress vector component. In the case where both axial and torsional loading are applied in-phase, the loading history (ψ) seen in Fig. 1 is a straight line, for this reason the τ_a is simply half of this straight line. The experimental data provided by Endo and Ishimoto (2006) have both in-phase and out-out-phase cases, and an adapted version of the MWCM will be assessed against these data produced for specimens containing small defects.

The critical plane, which lies in the coordinates (ϕ_c, θ_c), was originally defined by Susmel and Lazzarin (2002) as the one containing the maximum shear stress vector amplitude. However, this definition is imperfect, since there is always more than one plane where the shear stress amplitude is equal. For this reason, in the present paper, the critical plane definition used will be the one formulated by Araújo et al (2011). In this definition, the critical plane is chosen by defining a 1% tolerance over the maximum shear stress amplitude. Then, the plane containing the maximum normal stress among those with a candidate plane (ϕ^*, θ^*) that lies within the 1% tolerance interval for the shear stress amplitude, is chosen. In other words:

- Step 1: Find τ_a^{max}:

$$\tau_a^{max} = \max_{\phi,\theta}\{\tau_a(\phi, \theta)\} \tag{9}$$

- Step 2: Select candidate planes within 1% interval over τ_a^{max} ($tol = \tau_a^{max} \times 1\%$) :

$$(\phi^*, \theta^*) = \{(\phi, \theta): \tau_a^{max} - tol \leq \tau_a \leq \tau_a^{max}\} \tag{10}$$

- Step 3: Among the (ϕ^*, θ^*) set, identify the element with the maximum $\sigma_{n,max}$ to be the critical plane:

$$(\phi_c, \theta_c) = \max_{\phi^*,\theta^*}\{\sigma_{n,max}(\phi^*, \theta^*)\} \quad (11)$$

Adapting the MWCM to materials containing small defects

To extend the application of the MWCM criterion to estimate the limit of resistance of multiaxial fatigue in materials containing small defects (Neto, 2018), the following procedure is proposed:

I. Determine hardness of the material and the $\sqrt{area}$ parameter;
II. Estimate the axial fatigue strength (f_{-1}) according to Murakami's model (Eq. (1));
III. Estimate the torsional fatigue strength (t_{-1}) according to Murakami's model (Eq. (2));

Steps number II and III are key. By setting $f_{-1} = \sigma_w$ and $t_{-1} = \tau_w$, where σ_w is calculated by Eq. 1 and τ_w by Eq. 2, the effect of a surface defect is introduced into the MCWM.

IV. Determine λ and κ from f_{-1} and t_{-1} estimated in the step II and III;
V. Assess the accuracy of the new adapted MWCM for defective materials considering the available data.

Data available in the literature (Endo and Ishimoto, 2006)

The evaluation of the methodology was conducted with the data provided in the literature by Endo and Ishimoto (2006) in Figure 3. The exact values of the shear stress amplitude and the normal stress amplitude of each data point were extracted digitally. Specimens were subject to combined axial and torsional loads in servo-hydraulic driven testing machines. It was considered that the fatigue limit was the threshold stress condition that the specimen lasted for 10^7 cycles. Once runout value of 10^7 was reached without total specimen failure, the drilled holes where examined under a microscope and if micro fractures where detected, it was considered that these specimens had reached the fatigue limit threshold condition. In the experiments, two different types of steels were tested, the JIS S35C and the JIS SCM435, their properties are summarized in Table 1. Each material was tested under in-phase and out-of-phase loading. Defects were drilled with either $d = h = 100\ \mu m$ or $d = h = 500\ \mu m$, where d is their diameter and h their depth.

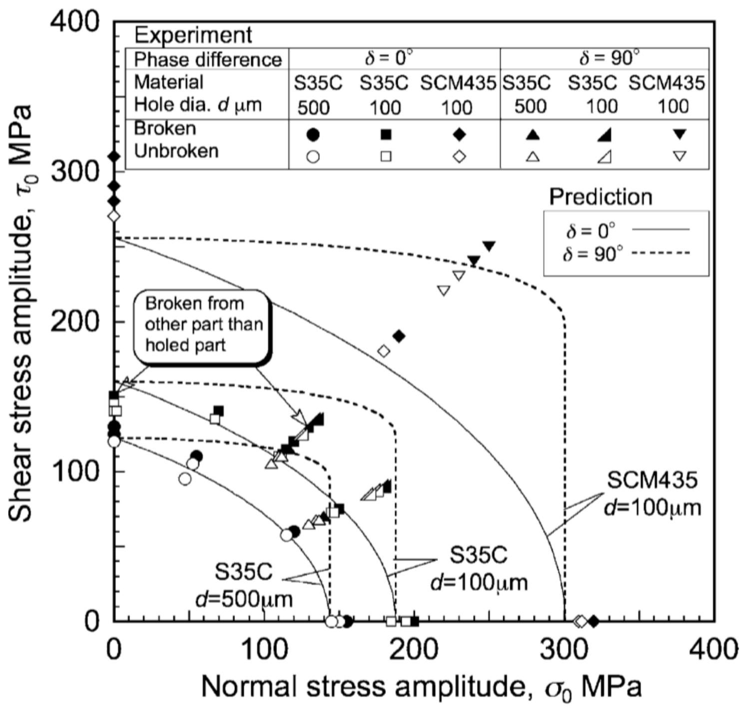

Figure 3 - Experimental data provided by Endo and Ishimoto (2006).

Table 1 - Properties of JIS S35C and of JIS SCM435 (Endo and Ishimoto, 2006)

Material	Lower yield point (MPa)	Tensile strength (MPa)	Reduction in area (%)	Vickers hardness (HV)
S35C	328	586	50.7	160
SCM435	853	948	65.0	327

RESULTS

In order to assess the proposed adaptation of the MWCM, its material constants κ and λ must be estimated according to the defect size. In order to do so, first, the equivalent $\sqrt{area}_{100}$ and $\sqrt{area}_{500}$ for holes with $d = h = 100\ \mu m$ and $d = h = 500\ \mu m$ respectively, need to be calculated. For this, Equation (12) was used (Endo and Ishimoto, 2006):

$$\sqrt{area} = \sqrt{d\left(h - \frac{d}{4\sqrt{3}}\right)} \tag{12}$$

Therefore, if $d = h = 100\ \mu m$:

$$\sqrt{area}_{100} = \sqrt{100\left(100 - \frac{100}{4\sqrt{3}}\right)} = 92.5\ \mu m \tag{13}$$

and if $d = h = 500\ \mu m$:

$$\sqrt{area}_{500} = \sqrt{500\left(500 - \frac{500}{4\sqrt{3}}\right)} = 462.5\ \mu m \tag{14}$$

In the torsional loading cases, the values of $\sqrt{area}_{100}$ and $\sqrt{area}_{500}$ had to be multiplied by $\cos 45°$, which is the angle of the principal stresses' plane for torsion. Moreover, the aspect ratio of the drilled holes (a/b) was 0.5 in every case, because $d = h$ always. Therefore, from Eq. (3) $F = 0.7097$.

With the values of Eq. (13) and Eq. (14), the fatigue limits σ_w and τ_w were calculated according to Eq. (1) and Eq. (2) and introduced in Table 2.

Table 2 - Values of τ_w and σ_w for each material and each defect type.

	$\tau_w\ (MPa)$		$\sigma_w\ (MPa)$	
	$d = 100\ \mu m$	$d = 500\ \mu m$	$d = 100\ \mu m$	$d = 500\ \mu m$
S35C	192.1	146.9	188.3	144.0
SCM435	306.6	-	300.6	-

With values of τ_w and σ_w, the constants κ and λ were calculated with Eq. (8) and the results introduced in Table 3.

Table 3 - MWCM model constants λ and κ for each defect size and material.

The $\sqrt{area}$ of the defect (μm)	S35C		SCM435	
	κ	λ	κ	λ
92.5	97.9	192.1	156.3	306.6
462.5	74.9	146.9	-	-

Figures 1, 2 and 3 show the fatigue strength curve of the corrected MWCM model (continuous blue line) for steels S35C and SCM435 for different sizes of defects and different load phases. Two dashed error lines of 10% and -10% for comparison were plotted as well. Points marked with a circle are the experimental points corresponding to specimens that did not break completely, only fractured at the defect's vicinities after running 10^7 cycles; while points marked with an 'x' are experimental points corresponding to the cases where the specimen failed completely.

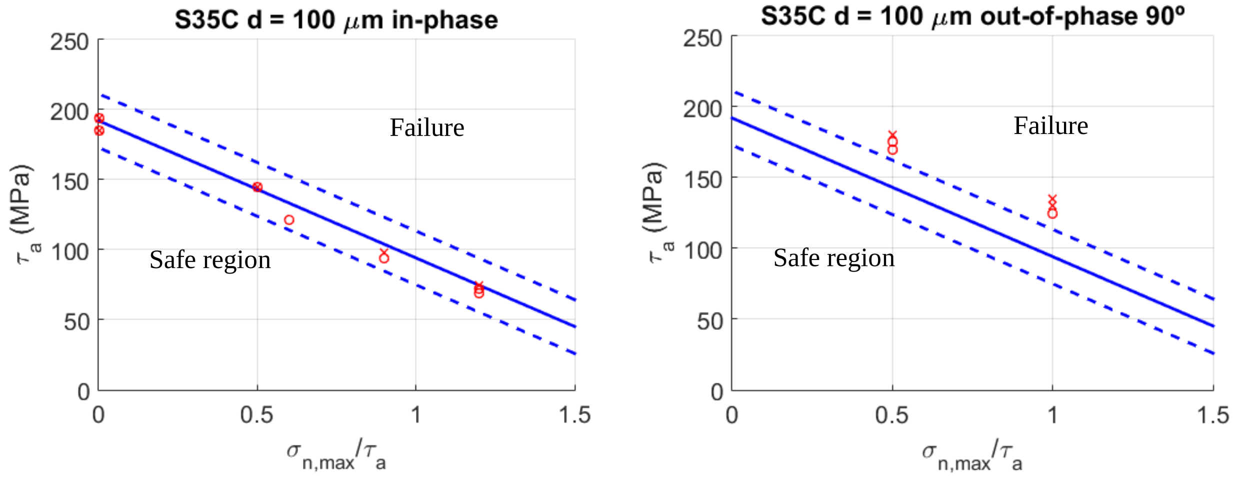

Figure 4 – MWCM diagrams for S35C with defect of $d = 100\ \mu m$ and (a) in-phase loading; (b) out-of-phase loading with 90º. Adapted from Endo and Ishimoto (2006).

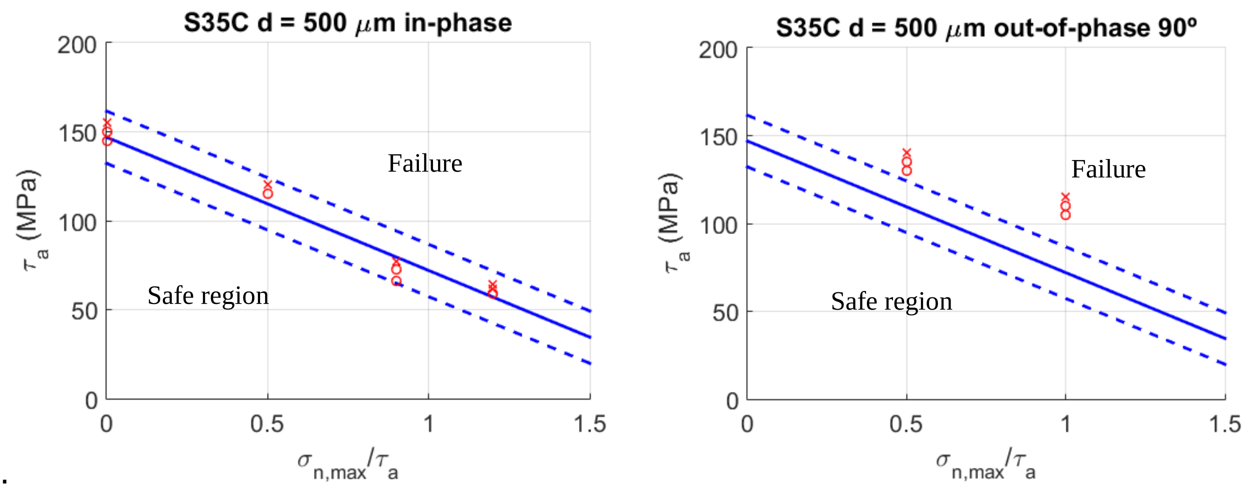

Figure 5 – MWCM diagrams for S35C with defect of $d = 500\ \mu m$ and (a) in-phase loading; (b) out-of-phase loading with 90º. Adapted from Endo and Ishimoto (2006).

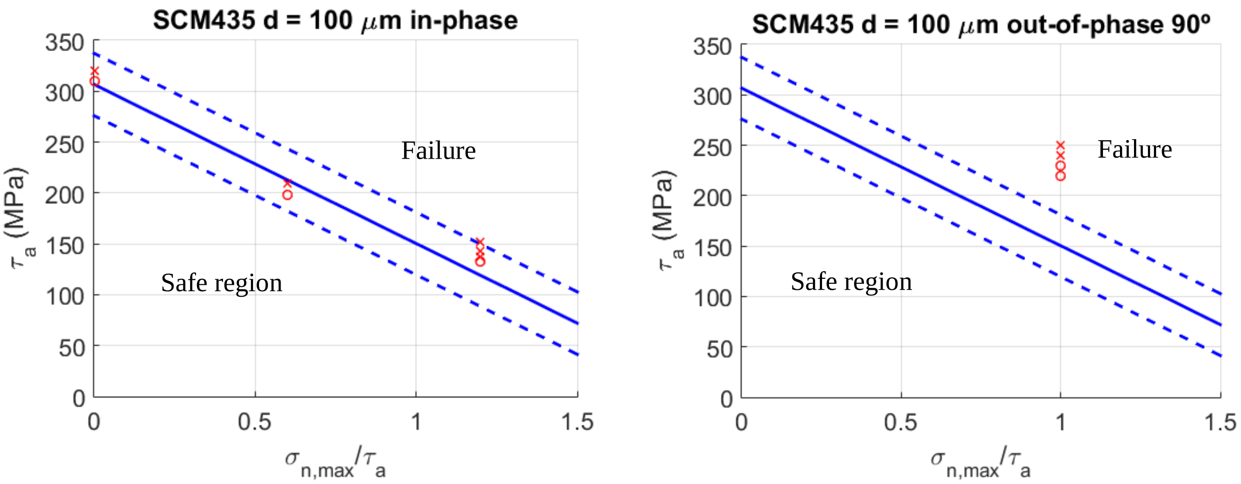

Figure 6 - MWCM diagrams for SCM435 with defect of $d = 100\ \mu m$ and (a) in-phase loading; (b) out-of-phase loading with 90º. Adapted from Endo and Ishimoto (2006).

Model assessment

Equation (15) is commonly used to calculate the prediction error index (EI%) and assess multiaxial fatigue criteria. By comparing the relative size of experimental result value (R_E) to the predicted result value (R_P) an error index (EI) is cauculated.

$$EI = \frac{R_E - R_P}{R_P} \times 100\% \tag{15}$$

As the model used in the current paper is the MWCM, as presented previously, Equation (15) can be rewritten as shown in Equation (16)

$$EI = \frac{\tau_a(\theta_c, \phi_c) + \kappa \frac{\sigma_{n,max}}{\tau_a}(\theta_c, \phi_c) - \lambda}{\lambda} \times 100\% \tag{16}$$

To understand how this error index is calculated, consider the experimental point from Figure 3 $(\sigma_0, \tau_0) = (180, 180)\ MPa$, which represents the applied amplitude of stresses on the specimen made of SCM435 and a defect of $d = 100\ \mu m$. First, the maximum amplitude of the shear stress (τ_a) and the maximum normal stress ($\sigma_{n,max}$) for this loading case must be calculated using the method described previously. The result is $(\sigma_{n,max}, \tau_a) = (123, 199)\ MPa$. Second, the constants λ and κ for the defect size and material must be calculated. The result is in Table 3. Finally, EI shall be calculated. In this specific case, it is -3,7%. Negative values of EI indicate a non-conservative prediction while positive values indicate a conservative prediction.

CONCLUSIONS

In this work an adapted version of the Modified Wöhler Curve Method (Susmel and Lazzarin, 2002) was proposed. The model was applied to evaluate the fatigue limit of specimens made of S35M and SCM435 steels containing small artificial holes and subjected to multiaxial loading (Endo and Ishimoto, 2006). To adapt the model we introduced the $\sqrt{area}$ parameter proposed by Murakami (2002a, (2002b) to estimate the material constants κ and λ from the nominal fatigue limits of these steels under uniaxial and torsional cyclic loading. The main advantage of Murakami's models is their capability predicting the nominal fatigue strength of hard steels containing microscopic defects with relative ease, as estimating the parameter $\sqrt{area}_{max}$ of a steel is a simple process (Murakami, 1994). In this context, it was shown that:

1. It is possible to determine the material constants of a multiaxial fatigue model such as the MWCM without necessarily having to run fatigue tests, which are lengthy and expensive.
2. The $\sqrt{area}$ parameter allowed to predict the multiaxial fatigue strength with precision mostly around 10% for the data provided by Endo and Ishimoto (2006).
3. The proposed model's predictions for in-phase combined loading were very good, as the error (EI%) remained mostly between -10% and 10% as can be seen in Figures 4 to 6.
4. Predictions for combined out-of-phase loading were very conservative, with the error mostly above 15%.

REFERÊNCIAS

Araújo, J. A., Dantas, A. P., Castro, F. C., & Mamiya, E. N. (2011). On the characterization of the critical plane with a simple and fast alternative measure of the shear stress ambplitude in multiaxial fatigue. *International Journal of Fatigue*, 1092-1100.

Bernasconi, A. (2001). Efficient algorithms for calculation of shear stress amplitude and amplitude of the second invariant of the stress deviator in fatigue criteria applications. 649-657.

Endo, M., & Ishimoto, I. (24 de Maio de 2006). The fatigue strength of steels containing small holes under out-of-phase combined loading. *International Journal of Fatigue*, pp. 592-597.

Fatemi, A., & Socie, D. F. (1988). A Critical Plane Approach to Multiaxial Fatigue Damage Including Out-of-Phase Loading. *Fatigue & Fracture of Engineering Materials and Strutures*, 149-165.

Findley, W. N. (1959). A theory for the effect of mean stress on fatigue of metals under combined torsion and axial load or bending.

Murakami, Y. (Julho de 1994). Inclusion Rating by Statistics of Extreme Values and Its Applications to Fatigue Strength Prediction and Quality Control of Materials. *Journal of Research of the National Institute of Standards and Technology*, pp. Volume 99, Número 4.

Murakami, Y. (2002a). Effect of Hardness Hv on Fatigue Limits of Materials Containing Defects, and Fatigue Limit Prediction Equations. Em *Metal Fatigue: Effects of Small Defects and Nonmetallic Inclusions* (pp. 57-74). Oxford: Elsevier.

Murakami, Y. (2002b). Torsional Fatigue. Em *Metal Fatigue: Effects of Small Defects and Nonmetallic Inclusions* (pp. 247-272). Oxford: Elsevier.

Murakami, Y., & Endo, M. (1994). Effects of Defects, inclusions and inhomogenities on fatigue strength. *International Journal of Fatigue*, 163-182.

Nadot, Y., & Billaudeau, T. (2006). Multiaxial fatigue limit criterion for defective materials. *Engineering Fracture Mechanics*, 112-133.

Neto, E. S. (2018). Avaliação de modelos multiaxiais para estimativa da resistência à fadiga de aços naturalmente defeituosos. *ENM.DM-282/218*. Brasília: Departamento de Engenharia Mecânica, Universidade de Brasília.

Schönbauer, B. M., & Yanese, K. (Junho de 2016). Influence of intrinsic and artificial defects on the VHCF properties of 17-HP stainless steel. *Procedia Structural Integrity*, 1149-1155.

Smith, K. N., Watson, P., & Topper, T. H. (1970). A Stress-Strain Function for the Fatigue of Metals. *Journal of Materials*, 767-778.

Susmel, L., & Lazzarin, P. (2002). A bi-parametric Wöhler Curve for High Cycle Multiaxial Fatigue Assesment. *Fatigue & Fracture of Engineerig Materials and Structures*, 63-78.

Yamashita, Y., Murakami, T., Mihara, R., Masami, O., & Murakami, Y. (2018). Defect analysis and fatigue design basis for Ni-based superalloy 718 manufactured by selective laser melting. *International Journal of Fatigue*, 485-495.

Yanase, K., & Endo, M. (1 de Abril de 2014). Multiaxial high cycle fatigue threshold with small defects nd cracks. *Engineering Fracture Mechanics*, pp. 182-196.